ARTICLE

Deletion of TLR4 attenuates lipopolysaccharide-induced acute liver injury by inhibiting inflammation and apoptosis

Sai-nan Chen[1,2], Ying Tan[3], Xiao-chan Xiao[2], Qian Li[2], Qi Wu[4], You-you Peng[5], Jun Ren[6,7] and Mao-long Dong[4]

Septic acute liver injury is one of the leading causes of fatalities in patients with sepsis. Toll-like receptor 4 (TLR4) plays a vital role in response to lipopolysaccharide (LPS) challenge, but the mechanisms underlying TLR4 function in septic injury remains unclear. In this study, we investigated the role of TLR4 in LPS-induced acute liver injury (ALI) in mice with a focus on inflammation and apoptosis. Wild-type (WT) and TLR4-knockout (TLR4$^{-/-}$) mice were challenged with LPS (4 mg/kg) for 6 h. TLR4 signaling cascade markers (TLR4, MyD88, and NF-κB), inflammatory markers (TNFα, IL-1β, and IL-6), and apoptotic markers (Bax, Bcl-2, and caspase 3) were evaluated. We showed that LPS challenge markedly increased the levels of serum alanine aminotransferase (ALT)/aspartate aminotransferase (AST) and other liver pathological changes in WT mice. In addition, LPS challenge elevated the levels of liver carbonyl proteins and serum inflammatory cytokines, upregulated the expression of TLR4, MyD88, and phosphorylated NF-κB in liver tissues. Moreover, LPS challenge significantly increased hepatocyte apoptosis, caspase 3 activity, and Bax level while suppressing Bcl-2 expression in liver tissues. These pathological changes were greatly attenuated in TLR4$^{-/-}$ mice. Similar pathological responses were provoked in primary hepatic Kupffer cells isolated from WT and TLR4$^{-/-}$ mice following LPS (1 μg/mL, 6 h) challenge. In summary, these results demonstrate that silencing of TLR4 attenuates LPS-induced liver injury through inhibition of inflammation and apoptosis via TLR4/MyD88/NF-κB signaling pathway. TLR4 deletion confers hepatoprotection against ALI induced by LPS, possibly by repressing macrophage inflammation and apoptosis.

Keywords: sepsis; acute liver injury; LPS; TLR4; inflammation; apoptosis; TLR4$^{-/-}$ mice; primary hepatic Kupffer cells

INTRODUCTION

Sepsis or septic shock constitutes a life-threatening condition known as multiple organ dysfunction syndrome that is caused by an uncontrolled host immune reaction to infection [1, 2]. At present, sepsis is the most frequent cause of fatalities in intensive care units [3]. The liver plays an array of vital roles in many physiological and pathophysiological processes, including detoxification, metabolism, immunity, and homeostasis, which makes this organ extremely vulnerable to endotoxin-induced damage during sepsis [4]. Sepsis-induced acute liver injury (ALI) is one of the leading causes of death among patients afflicted with sepsis. Patients with ALI exhibit clinical manifestations ranging from mild increases in liver enzymes to severe liver failure. Liver injury due to sepsis directly leads to disease progression and death [5]. Numerous mechanisms have been suggested to underscore the etiology of sepsis-induced ALI, including inflammatory and immune responses, cellular hypoxia, apoptosis, and oxidative stress [6]. However, the precise mechanism underlying the onset and progression of sepsis-associated liver damage remains unclear. Through improvements in intensive care management, the survival rate of sepsis patients has improved markedly in

recent years. However, the search for more effective therapeutic regimens for sepsis-induced ALI remains challenging.

Several studies have shown that the lipopolysaccharide (LPS) produced by gram-negative bacteria induces sepsis, which may progress into systemic organ failure, including liver dysfunction [7–9]. The association between liver injury and LPS-induced endotoxemia has been confirmed in various experimental animal models [10]. The liver is the most crucial detoxification and immune organ in the human body, and LPS directly acts as a liver endotoxin, causing liver damage. In addition, LPS activates hepatic macrophages, including Kupffer cells, to secrete inflammatory cytokines and induces hepatocyte necrosis or apoptosis, ultimately resulting in liver injury [11, 12]. Herein, we demonstrated that host innate immunity is tightly associated with the inflammatory response and apoptosis and promotes sepsis-induced ALI. However, the effect of inflammation and apoptosis on sepsis-induced liver injury has not been explored. Toll-like receptor 4 (TLR4) is the core mediator of adaptive and innate immune reactions to LPS [13]. TLR4 facilitates molecular recognition of trace amounts of endotoxins in the circulation, dimerizes receptors on cell membranes, and initiates a cascade of

[1]Department of Critical Care Medicine, Zhujiang Hospital, Southern Medical University, Guangzhou 510282, China; [2]Department of Emergency Medicine, Nanfang Hospital, Southern Medical University, Guangzhou 510515, China; [3]Department of Critical Care Medicine, Nanfang Hospital, Southern Medical University, Guangzhou 510515, China; [4]Department of Burns, Nanfang Hospital, Southern Medical University, Guangzhou 510515, China; [5]Shanghai Hongrun Boyuan School, Shanghai 201713, China; [6]Department of Cardiology, and Shanghai Institute of Cardiovascular Diseases, Zhongshan Hospital Fudan University, Shanghai 200032, China and [7]Department of Laboratory Medicine and Pathology, University of Washington, Seattle, WA 98195, USA
Correspondence: Jun Ren (jren_aldh2@outlook.com) or Mao-long Dong (2206723777@qq.com)
These authors contributed equally: Sai-nan Chen, Ying Tan

Lipopolysaccharide, TLR4, and acute liver injury
SN Chen et al.

1611

protein–protein interactions. These interactions produce proinflammatory cytokines and interferons that trigger inflammation and immune responses in the context of bacterial sepsis [14, 15]. While primarily expressed in macrophages, TLR4 is also expressed in other types of cells, including hepatocytes [16]. Ample evidence has indicated a vital role for TLR4 signaling in various pathological conditions in the liver, including hepatic steatosis, liver fibrosis, liver failure, and inflammatory liver diseases [17–19]. Moreover, LPS binds to LPS-binding proteins to form complexes with MD2 and CD14, which are recognized by TLR4 in the Kupffer cell membrane. This activated receptor complex transmits TLR4 signals through specialized intracellular proteins, including myeloid differentiation factor 88 (MyD88), tumor necrosis factor (TNF) receptor-associated factor, and interleukin-1 receptor-associated kinases, triggering activation of the NF-κB cascade and the induction of a multifaceted cellular response network, such as the secretion of various inflammatory factors [TNF-alpha (TNF-α), IL-6, IL-1β] and the production of granulocyte-macrophage colony-stimulating factor. This series of reactions induces hepatocyte apoptosis or necrosis, eventually leading to irreversible liver damage [20].

In the present study, we hypothesized that the TLR4/MyD88/NF-κB signaling pathway participates in LPS-induced liver injury and that the underlying mechanisms involved inflammation and apoptosis. Hepatic biochemical tests were conducted on sera from wild-type and TLR4-knockout mice following LPS administration. TLR4 signaling molecules, inflammatory factors, and apoptotic protein markers were also evaluated.

MATERIALS AND METHODS

Chemicals and reagents
LPS (*Escherichia coli*, 055: B5) was obtained from Sigma (Santa Clara, CA, USA). Dulbecco's modified Eagle's medium and fetal bovine serum (FBS) were purchased from Gibco (Grand Island, NY, USA). The cell counting kit-8 (CCK-8) assay, cell cycle detection kit, and Annexin V-FITC/(propidium iodide)PI apoptosis kit were purchased from Dojindo Laboratories (Kumamoto, Japan). PE-F4/80 and FITC-CD11b antibodies were purchased from Biolegend Inc. (San Diego, CA, USA). The protein oxidative carbonyl test kit was acquired from Solarbio (Beijing, China). The cysteinyl aspartate specific proteinase 3 (caspase 3) activity detection kit was purchased from BestBio (Shanghai, China). Anti-Bax (catalog #2772), anti-Bcl-2 (catalog #2876S), anti-TLR4 (catalog #14358), anti-MyD88 (catalog #4283), anti-NF-κB (catalog #8242), anti-p-NF-κB (catalog #3033), and anti-GAPDH were obtained from Cell Signaling Technology (Boston, MA, USA). RNAiso Plus, the PrimeScript™ RT reagent kit, and the SYBR Premix Ex Taq kit were procured from Takara (Dalian, China).

Experimental animals and LPS administration
C57BL/10J mice and TLR4$^{-/-}$ mice were purchased from GemPharmatech Co., Ltd. All animal experiments conducted in this study were approved by the Animal Care and Use Committees of Nanfang Hospital, Southern Medical University (Guangzhou, China). Before the experiment, all mice were kept in specific pathogen-free level animal housing in the Animal Laboratory Center. The animals were allowed free access to water and food in a climate-controlled environment (24 °C, humidity 50%–60%) with a 12-h/12-h light/dark cycle. Genotyping of TLR4-knockout (TLR4-KO or TLR4$^{-/-}$) mice was performed using PCR. Adult WT and TLR4$^{-/-}$ mice were administered LPS (4 mg/kg) or saline for 6 h, as described previously [21].

Isolation of primary murine Kupffer cells
Primary Kupffer cells were isolated from mice using the in situ collagenase (Type VI; Sigma-Aldrich) perfusion technique, as previously described with modifications [22, 23]. Briefly, livers were perfused with Ca^{2+}- and Mg^{2+}-free HBSS (Gibco, Grand Island, NY, USA) containing 0.1 mM EGTA for 10 min at 37 °C, followed by reperfusion with liver digestion fluid [HBSS containing 15 mM HEPES, 5 mM CaCl$_2$, and 0.1 mg/mL collagenase IV (Sigma, Santa Clara, CA, USA)] for an additional 10 min. The liver was then removed and placed in a culture dish containing HBSS and gently shaken to collect the digested cells. Cell suspensions were filtered through a sterile 70-µm nylon cell strainer (BD, Franklin Lake, NJ, USA) to remove undigested and connective tissues. The cells were centrifuged for 3 min at 50 × g (4 °C). The supernatant containing Kupffer cells was centrifuged at 500 × g for 5 min (4 °C) to collect the pellets, which were then resuspended in HBSS and subjected to two-step Percoll gradient (25%/50%) centrifugation at 1300 × g for 20 min (4 °C). Cells were collected from the 25% to 50% Percoll gradients, rinsed and cultured in RPMI-1640 supplemented with 10% FBS and 1% penicillin-streptomycin for 2 h. Nonadherent cells were removed by replacing the medium prior to experimentation.

Flow cytometric analysis of macrophage purity and apoptosis
The percentage of F4/80- and CD11b-positive cells was determined using flow cytometry. Briefly, a Kupffer cell suspension was obtained by digestion with 0.25% trypsin for 5 min, and the precipitate was obtained by centrifugation at 800 r/min for 5 min and then incubated with 10% normal goat serum to block nonspecific protein–protein interactions. The cells were then incubated with the antibody of interest (1:100 dilution) at 22 °C for 30 min. For the apoptosis assay, an Annexin V-FITC/PI apoptosis kit and cell cycle detection kit were used to assess the level of apoptosis in macrophages. For apoptosis detection, cells were rinsed in PBS after drug treatment and were then resuspended in a combination buffer containing FITC reagent before being incubated in the dark at room temperature for 15 min. Finally, PI was added to cells. The data were collected using a flow cytometer (Beckman Coulter, California, CA, USA) and were analyzed using FlowJo software.

Cell viability assay
We seeded primary Kupffer cells into 96-well plates, and the adherent cells were cultured for 24 h. Next, the cells were exposed to 100 µL of culture medium supplemented with or without LPS (1 µg/mL) for 6 h. Drug-free medium served as the control. Finally, we added CCK-8 reagent (10 ng/mL) to the cells and incubated them for 3 h. Then, we measured the absorbance of the enzyme marker at 450 nm to determine the cell viability. The cell inhibition rate was calculated as described previously [20].

Biochemical analysis
Blood samples were collected by cardiac puncture and centrifuged at 3000 r/min for 15 min using a high-speed centrifuge to obtain serum. Serum alanine aminotransferase (ALT) and aspartate aminotransferase (AST) levels were measured using ALT and AST assay kits (Jiancheng, Nanjing China), respectively [24].

Histopathology
Fresh liver tissues were first fixed with 4.0% formalin buffer for 24 h to stabilize the tissue. Paraffin embedding was performed using standard techniques. Sections with a thickness of 4 µm were stained with hematoxylin and eosin and then observed under a microscope. The pathological scores of liver tissues were calculated as described by Suzuki et al. [25]. The scoring parameters included congestion, edema, cytoplasmic vacuolization, and necrosis of hepatic cells. The highest possible score was 4 points.

TUNEL staining
To examine cell apoptosis in liver tissues, a TUNEL staining kit (Beyotime, Shanghai, China) was used to stain paraffin sections of liver tissues according to the protocol provided by the

1612

manufacturer. Moreover, hepatocyte nuclei were stained with DAPI (blue). Cells in the liver sections were visualized with a fluorescence microscope at a magnification of ×40 [26].

Enzyme-linked immunosorbent assay (ELISA)
Serum and supernatant levels of TNF-α, IL-6, and IL-1β were analyzed using ELISA kits (R&D Systems, Minneapolis, MN, USA) according to the instructions of the manufacturer.

Carbonyl assay
To determine the levels of oxidative proteins in mouse livers, hepatic protein carbonyl levels were analyzed using a carbonyl protein detection kit (Solarbio, Beijing, China) according to the manufacturer's procedure. Briefly, tissue samples were finely minced in lysis buffer. The supernatant containing the proteins was collected after centrifugation at $5000 \times g$ for 10 min. Next, the proteins were incubated in the reaction buffer in the dark at 37 °C for 1 h and were then precipitated by the addition 20% trichloroacetic acid solution. We further incubated the precipitate at room temperature for 15 min, followed by centrifugation at 12 000 × g for 10 min at 4 °C. After that, the precipitate was washed three times. Finally, 6 M guanidine HCl was added to dissolve the pellets, followed by incubation at 37 °C for 30 min. After the precipitate was completely dissolved, the solution was centrifuged at 12,000 × g for 15 min. The maximum absorbance (370 nm) of the supernatant was measured and compared to the corresponding blanks, and the carbonyl level was calculated using the molar absorption coefficient of 22000 mol/L per cm [27].

Caspase 3 assay
To determine the rate of apoptosis in liver cells, the enzymatic activity of apoptosis-induced caspase 3 was measured with a caspase 3 assay kit (BestBio, Shanghai, China) according to the manufacturer's protocol. Briefly, tissue samples were finely minced in lysis buffer and incubated at room temperature for 15 min. Next, the supernatant was collected after centrifugation at 12,000 × g for 15 min at 4 °C. Caspase 3 activity was measured in a 96-well plate, and each well contained 50 μL of lysate, 40 μL of assay buffer, and 10 μL of caspase 3 colorimetric substrate reagent. The plate was incubated at 37 °C for 4 h. Finally, the absorbance of each well was measured at 405 nm using a microplate reader. Protein levels were estimated using the BCA method [28].

Determination of NF-κB expression in liver tissue using immunohistochemistry
Briefly, sections of liver tissues were dewaxed prior to dehydration. Next, 3% H_2O_2 was used to eliminate endogenous peroxidase activity in the liver tissues, after which antigen repair was performed using the proteinase k method. Subsequently, liver sections were incubated with goat serum for 1 h and then with p-NF-κB (1:300) antibodies overnight at 4 °C. Next, we washed the sections with TBST three times and incubated them with a rabbit IgG secondary antibody at 37 °C for 60 min. The sections were developed with diaminobenzidine and then stained with hematoxylin to reveal the cell nuclei. The percentage of p-NF-κB-positive cells was determined using ImageJ software.

Quantitative real-time PCR to detect mRNA expression
Total RNA was extracted from primary Kupffer cells and liver tissues using an RNAiso Plus kit (Takara, Japan) according to the manufacturer's protocol. We reverse transcribed the isolated RNA into cDNA using the PrimeScript™ RT reagent kit (Takara, Japan). Next, qPCR was conducted using a SYBR Premix Ex Taq kit on a QuantStudio™ 5 system (Thermo, USA). The amplification conditions included initial denaturation at 95 °C for 10 s, followed by 40 cycles at 95 °C for 5 s and at 60 °C for 20 s. GAPDH was used as the control gene. The relative expression levels were estimated using

Table 1. RT-PCR primer sequences for TLR4, Myd88, NF-κB, TNF-α, IL-1β, and IL-6.

Primer		Sequence (5′ → 3′)
TLR4	Forward	ATGGCATGGCTTACACCACC
	Reverse	GAGGCCAATTTTGTCTCCACA
MYD88	Forward	TCATGTTCTCCATACCCTTGGT
	Reverse	AAACTGCGAGTGGGGTCAG
NF-κB	Forward	ATGGCAGACGATGATCCCTAC
	Reverse	TGTTGACAGTGGTATTTCTGGTG
TNF-α	Forward	GGACTAGCCAGGAGGGAGAACAG
	Reverse	GCCAGTGAGTGAAAGGGACAGAAC
IL-1β	Forward	CACTACAGGCTCCGAGATGAACAAC
	Reverse	TGTCGTTGCTTGGTTCTCCTTGTAC
IL-6	Forward	AGCCCACCAAGAACGATAGTCAATTC
	Reverse	GTCACCAGCATCAGTCCCAAGAAG
GAPDH	Forward	GGTTGTCTCCTGCGACTTCA
	Reverse	TGGTCCAGGTTTCTTACTCC

the 2$^{-\Delta\Delta Ct}$ method. The primers used were synthesized by Sangon (Shanghai, China), and the sequences are listed in Table 1 [28].

Western blotting
Protein extracts from whole cell and liver tissue samples were separated on SDS-PAGE gels and transferred onto polyvinylidene fluoride (PVDF) membranes (Millipore, Massachusetts, MA, USA). The membranes were blocked with 5% skimmed milk in Tris-buffered saline-Tween (TBST) for 1 h. After being blocked, the membranes were probed overnight at 4 °C with anti-TLR4 (1:1000), anti-MyD88 (1:1000), anti-NF-κB (1:1000), anti-p-NF-κB (1:1000), anti-caspase 3, anti-Bax (1:1000), anti-Bcl-2 (1:1000), and anti-GAPDH (1:10,000) antibodies. Subsequently, the PVDF membranes were washed three times in TBST and then incubated for 1 h at room temperature with HRP-labeled secondary antibodies. Protein bands were visualized using enhanced chemiluminescence reagents with GAPDH or β-actin as the internal control [28].

Statistical analysis
The data are presented as the mean ± SEM. Differences between multiple treatments were analyzed by analysis of variance (ANOVA), and the means were separated by Tukey's test (post hoc analysis). A value of $P < 0.05$ was considered statistically significant.

RESULTS
General biometric properties of WT and TLR4$^{-/-}$ mice
LPS administration had no effect on body weights (BWs) in any mouse group. In addition, TLR4 deficiency had no effect on body or organ weights. LPS markedly increased heart weight (HW) and liver weight (LW) and elevated the ratios of HW to BW (HW:BW) and LW to BW (LW:BW) ($P < 0.05$ vs. the WT group). However, the effect of LPS was alleviated by TLR4 deficiency (Table 2).

Effects of TLR4 deficiency on LPS-induced hepatic pathological and biochemical parameters
ELISA analysis of biochemical indices (ALT/AST) and carbonyl protein assays were conducted to explore the impact of TLR4 on LPS-induced brachy-chronic liver injury. We examined the functions and oxidative damage of liver tissues in each group. The results showed that serum ALT and AST levels and the expression of carbonyl protein in the liver, were significantly increased following LPS administration ($P < 0.05$ vs. the WT group),

Lipopolysaccharide, TLR4, and acute liver injury
SN Chen et al.

1613

although the effect of LPS was attenuated by TLR4 knockout. TLR4 deficiency had no impact on serum ALT or AST levels or carbonyl protein expression in the liver (Fig. 1c–e).

In the WT and TLR4$^{-/-}$ groups, the morphological structure of the liver lobules was clear, with liver cells exhibiting a neat architecture, normal size, and little inflammatory cell infiltration. However, in the WT-LPS group, the morphology of the hepatic lobules was abnormal, and the hepatocytes were disorderly arranged. Additionally, we observed marked necrosis of liver cells and scattered inflammatory cell infiltration. The structure of hepatic lobules in the livers of TLR4$^{-/-}$-LPS mice was clearer than that in the livers of WT-LPS mice. Moreover, inflammatory cell infiltration was decreased (Fig. 1a). The pathological score of liver tissues in the WT-LPS group was markedly higher ($P < 0.05$) than that in the WT group; however, the liver pathology score in the TLR4$^{-/-}$-LPS group was lower than that in the WT-LPS group ($P < 0.05$) (Fig. 1b).

Effects of TLR4 deficiency on LPS-induced changes in the TLR4/MyD88/NF-κB signaling pathway

The TLR4/MyD88 signaling pathway regulates NF-κB, a crucial intracellular modulator of inflammation and cell death in the liver

under different pathological conditions [29]. Hence, we examined the effect of TLR4 deficiency on the expression of TLR4 and MyD88 and the phosphorylation of NF-κB at 6 h following LPS administration ($n = 5$ or 6 per group). Consequently, LPS administration markedly upregulated the levels of TLR4, MyD88, and NF-κB phosphorylation. However, TLR4 knockout led to a marked decrease in LPS-induced TLR4, MyD88, and NF-κB activation ($P < 0.05$) (Fig. 2a–f). Furthermore, we conducted an immunohistochemical staining assay to assess the effect of TLR4 deficiency on the expression of p-NF-κB at 6 h following LPS administration. Compared with those of untreated-LPS mice, liver tissue sections of WT-LPS mice exhibited higher levels of p-NF-κB. However, TLR4 deficiency led to a marked reduction in the levels of nuclear p-NK-κB ($P < 0.05$).

Effects of TLR4 deficiency on LPS-induced changes in proinflammatory cytokines

Studies have shown that the overexpression of inflammatory cytokines is critically involved in the occurrence and development of LPS-associated ALI [7, 30]. Therefore, we performed ELISA and qPCR to examine the expression levels of TNF-α, IL-6, and IL-1β in the liver and serum (Fig. 3a–f). Consequently, TLR4 deficiency did not affect the levels of TNF-α, IL-1β, and IL-6 in the liver or serum ($P > 0.05$). However, compared to those of the WT group, the expression levels of IL-6, IL-1β, and TNF-α in the liver and serum were markedly increased after LPS administration ($P < 0.05$). In contrast, the levels of IL-1β, TNF-α, and IL-6 in the liver and serum were markedly decreased in the TLR4$^{-/-}$-LPS group compared with the WT-LPS group after LPS administration.

Effects of TLR4 deficiency on LPS-induced changes in hepatocyte apoptosis

Caspase 3 activity assays, TUNEL staining and Western blotting were performed to evaluate the impact of TLR4 deficiency on hepatocyte apoptosis (Fig. 4a–e). We hypothesized that TLR4 deficiency exerted hepatoprotective effects against LPS-induced
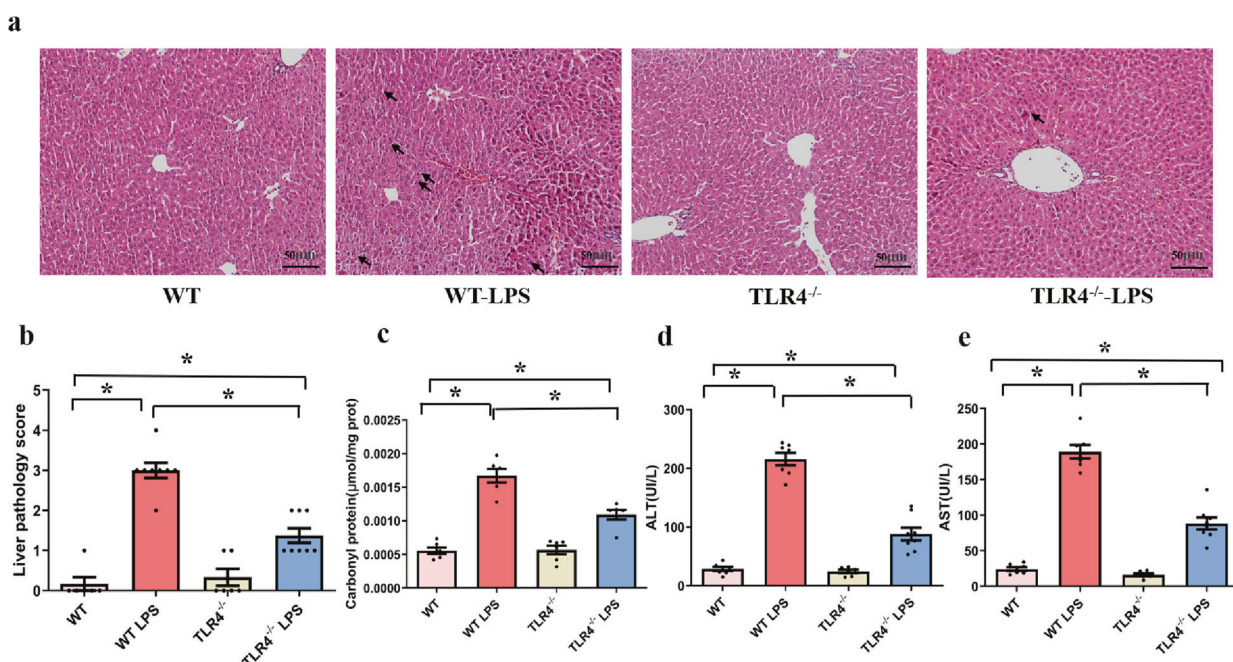
Table 2. Biometric parameters of WT and TLR4$^{-/-}$ mice treated with LPS or saline.

Parameter	WT	WT-LPS	TLR4$^{-/-}$	TLR4$^{-/-}$-LPS
Body weight (g)	24.1 ± 0.8	23.9 ± 0.7	24.1 ± 0.7	24.2 ± 0.8
Heart weight (mg)	132 ± 4	154 ± 7*	134 ± 4	139 ± 7#
Heart/body weight (mg/g)	5.50 ± 0.18	6.43 ± 0.31*	5.55 ± 0.17	5.75 ± 0.24#
Liver weight (g)	1.34 ± 0.05	1.52 ± 0.12*	1.33 ± 0.03	1.38 ± 0.05#
Liver/body weight (mg/g)	55.8 ± 2.0	63.5 ± 4.1*	54.9 ± 2.3	56.9 ± 3.0#

Mean ± SEM, $n = 10$–12 mice per group.
*$P < 0.05$ vs. WT group.
#$P < 0.05$ vs. WT-LPS group.

Fig. 1 Effect of TLR4 deficiency on LPS-induced hepatic pathological and biochemical parameters. Mice were challenged with saline or LPS (4 mg/kg, 6 h). **a** Liver samples were stained with H&E for histological assessment, and representative images from each group are shown (original magnification, ×200). **b** Histopathological scores. **c** Levels of oxidative carbonyl proteins in liver tissues in the groups. Serum levels of ALT (**d**) and AST (**e**) were measured at 6 h after intraperitoneal injection of LPS. Mean±SEM, $n = 6$–8 mice in each group; *$P < 0.05$ between the indicated groups.

Lipopolysaccharide, TLR4, and acute liver injury
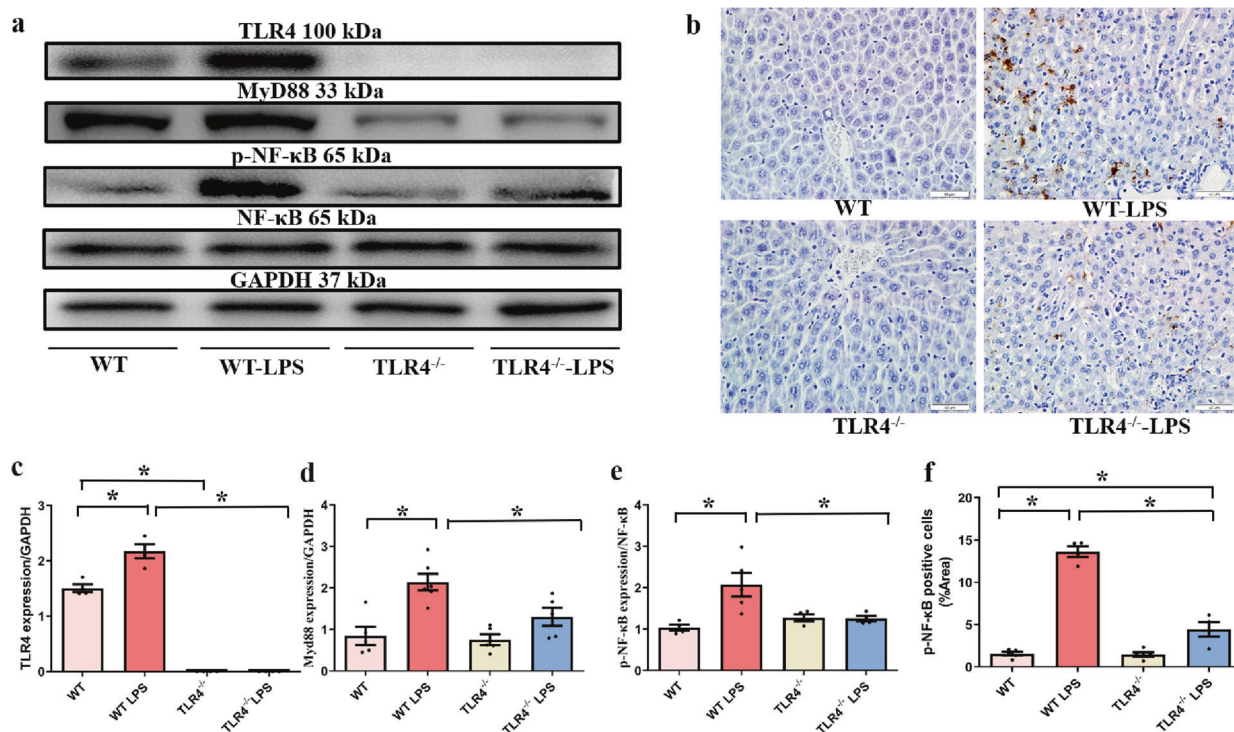SN Chen et al.

1614

Fig. 2 Western blot results showing the expression of TLR4 and its downstream targets and the IHC analysis results showing the level of NF-κB in liver tissue in the indicated groups. a Representative gel blots showing the levels of TLR4, MyD88, NF-κB, and p-NF-κB (GAPDH as the loading control). **b** Representative images showing the binding of p-NF-κB antibody and DAPI (original magnification, ×400). **c** TLR4 expression. **d** MyD88 expression. **e** NF-κB phosphorylation (p-NF-κB-to-NF-κB ratio). **f** Quantitative results showing p-NF-κB-positive cells. Mean±SEM, $n = 4$–8 mice in each group; $^*P < 0.05$ between the indicated groups.
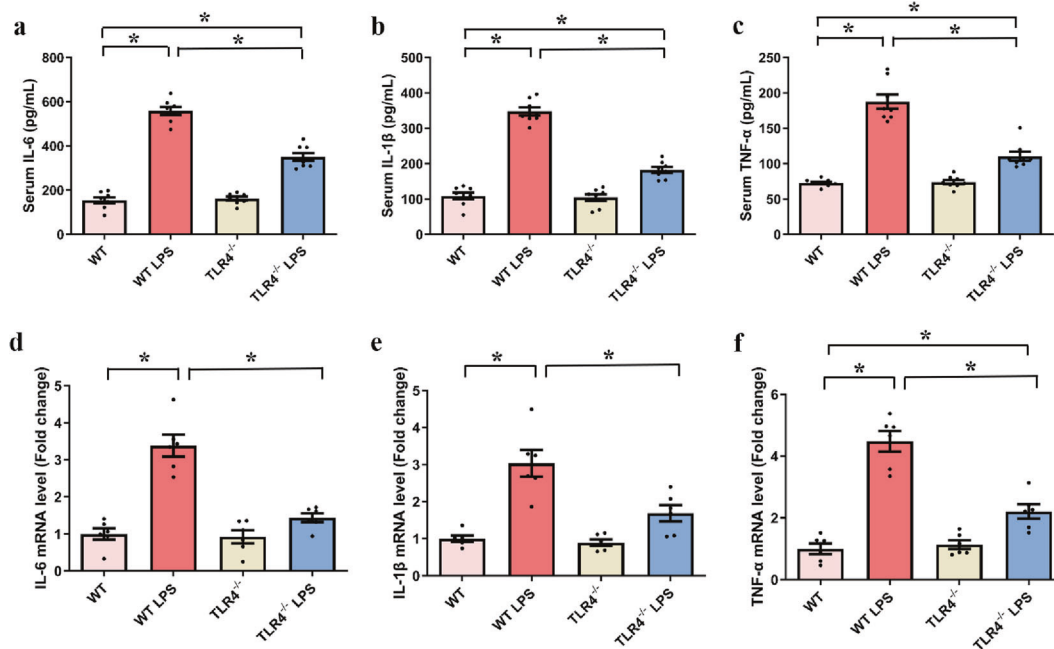

Fig. 3 Impact of TLR4 knockout (TLR4$^{-/-}$) on LPS-induced effects on hepatic and serum markers of inflammation. a Serum IL-6 levels. **b** Serum IL-1β levels. **c** Serum TNF-α levels. **d** Hepatic IL-6 mRNA levels. **e** Hepatic IL-1β mRNA levels. **f** Hepatic TNF-α mRNA levels. Mean ± SEM, $n = 4$–7 mice in each group; $^*P < 0.05$ between the indicated groups.

injury. LPS administration led to marked increases in caspase 3 activity, the number of TUNEL-positive cells, and the level of Bax, in association with a marked decrease in the level of Bcl-2 ($P < 0.05$ vs. the WT group), and these effects were attenuated by TLR4 deficiency. Notably, TLR4 deficiency did not directly influence these apoptotic biomarkers.
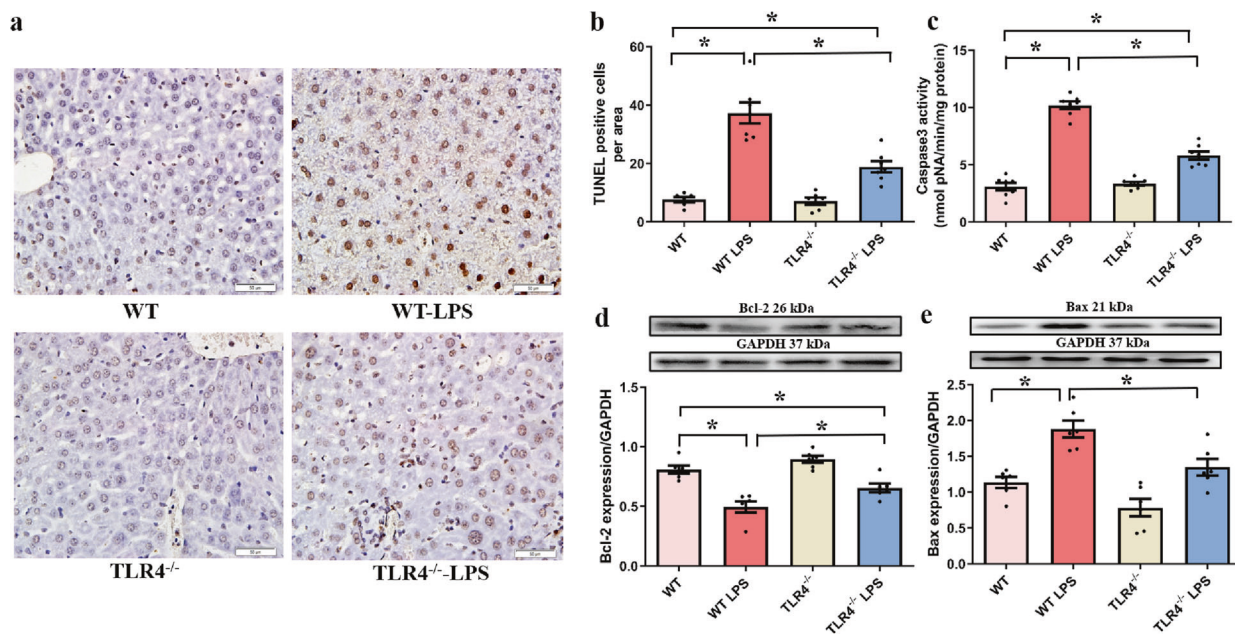
Lipopolysaccharide, TLR4, and acute liver injury
SN Chen et al.

1615

Fig. 4 **Impact of TLR4 knockout (TLR4$^{-/-}$) on LPS-induced hepatocyte apoptosis.** Apoptosis in hepatic tissues was determined by TUNEL assays, caspase 3 activity assays, and Western blotting, and the results show the expression of apoptosis-associated proteins. **a** Representative TUNEL staining images for each group (original magnification, ×400). **b** The number of TUNEL-positive cells in each group. **c** Caspase 3 activity. **d** Bcl-2 expression. **e** Bax expression. Mean ± SEM, $n = 6$–8 mice in each group; $^*P < 0.05$ between the indicated groups.

Effects of TLR4 deficiency on LPS-induced injury in primary liver macrophages in vitro

To examine the effect of TLR4 deficiency on LPS-induced acute injury in hepatic macrophages, Kupffer cells were isolated from the livers of WT and TLR4$^{-/-}$ mice. Cells were identified by flow cytometry after being labeled with specific antibodies in vitro. F4/80 and CD11b are the most commonly used markers for macrophages [31]. Based on our results, it was noted that the percentage of F4/80-positive cells was greater than 85%, which validated the high purity of the isolated primary macrophages. Moreover, the percentage of F4/80 and CD11b double-positive cells showed the levels of primary macrophage differentiation (Fig. 5a, b). LPS stimulation was used to establish a septic macrophage model. We next assessed the effect of TLR4 deficiency on LPS-induced cell viability using a CCK-8 assay. Our results indicated that LPS administration significantly reduced the viability of Kupffer cells, and the effect was mitigated by TLR4 deficiency ($P < 0.05$). TLR4 deficiency had little overt effect on cell morphology or viability in the absence of LPS challenge (Fig. 5c).

Effects of TLR4 deficiency on LPS-induced changes in the TLR4/MyD88/NF-κB signaling pathway in vitro

LPS elevated the protein and mRNA levels of TLR4 and MyD88 and the phosphorylation of NF-κB in primary Kupffer cells ($P < 0.05$ vs. the WT group). Intriguingly, this effect was abolished by TLR4 deficiency with little effect on TLR4 ablation itself (Fig. 6a–f).

Effects of TLR4 deficiency on proinflammatory cytokines following LPS administration in vitro

LPS administration significantly increased the protein and mRNA levels of TNF-α, IL-6, and IL-1β in primary Kupffer cells ($P < 0.05$ vs. the WT group), and the effect was abrogated by TLR4 deficiency with little effect on TLR4 ablation itself (Fig. 7a–f).

Effects of TLR4 deficiency on apoptotic proteins following LPS administration in vitro

LPS significantly elevated the total number of apoptotic cells, caspase 3 activity, and Bax expression. Moreover, LPS

downregulated the level of Bcl-2 in primary Kupffer cells ($P < 0.05$ vs. the WT group). TLR4 deficiency ablated these LPS-induced effects with little effect on apoptosis (Fig. 8a–d).

DISCUSSION

Sepsis-induced ALI is one of the most destructive types of organ dysfunctions associated with severe sepsis and induces serious health problems [32]. The mouse model of LPS-induced sepsis is an accepted animal model that has been used to study mechanisms related to ALI during sepsis [11, 12]. Notably, TLR4 signaling is crucially involved in sepsis-induced inflammatory and immune responses [7, 16]. Herein, a mouse model of LPS-induced sepsis was established to discern the potential effect of TLR4 expression on LPS-induced ALI in mice with sepsis.

In this study, TLR4 deficiency alleviated adverse changes in hepatic biochemical indices and liver morphology. In addition, TLR4 deficiency inhibited proinflammatory cytokine expression, as well as hepatic apoptosis, following LPS administration. These results suggest that TLR4 knockout protects against LPS-induced ALI by reducing inflammation. In particular, TLR4 mediates proinflammatory cytokine production and apoptosis. Importantly, our data showed that LPS-induced changes in the inflammatory response and hepatocyte apoptosis are tightly associated with activation of the TLR4 signaling cascade and the phosphorylation of NF-κB. Furthermore, the results of our in vitro experiment indicate that TLR4 knockout protects against Kupffer cell damage by suppressing inflammation and apoptosis. These results are consistent with the hypothesis that the TLR4 signaling pathway is vitally involved in altered susceptibility to LPS-induced macrophage inflammation and apoptosis in the context of TLR4 deficiency. Collectively, these findings reveal that TLR4 knockout protects against LPS-induced dysfunctional inflammatory responses, particularly TLR4/MyD88/NF-κB-mediated proinflammatory factor production and apoptosis, ultimately attenuating sepsis-induced ALI.

Several studies have reported the presence of unfavorable changes in hepatic liver enzymes and morphology during sepsis
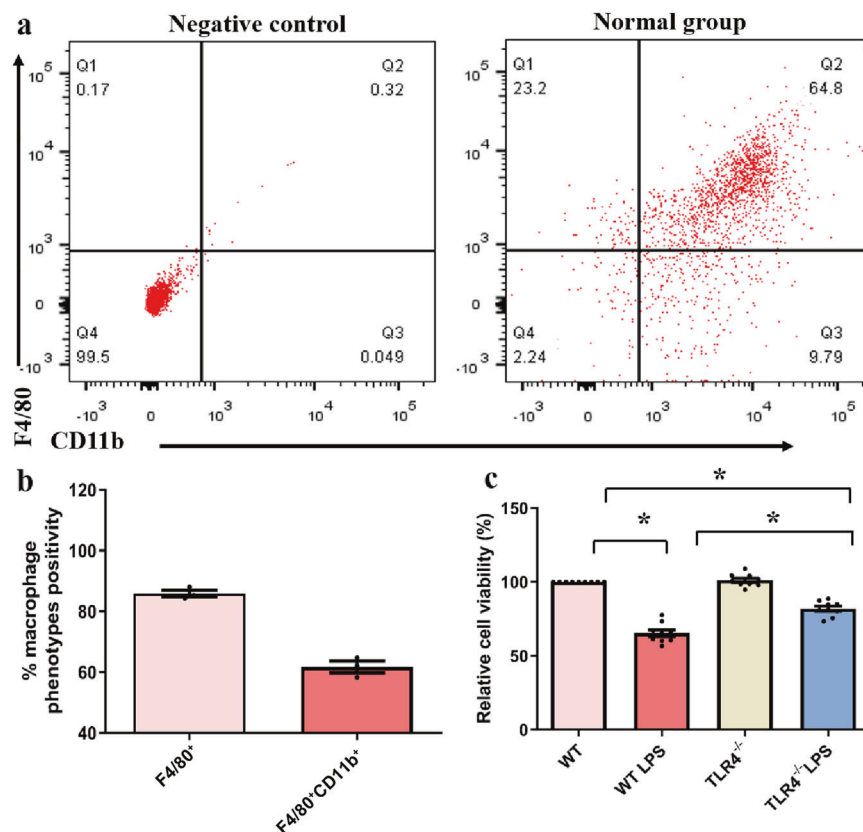
Lipopolysaccharide, TLR4, and acute liver injury
SN Chen et al.

1616

Fig. 5 Effect of TLR4 knockout (TLR4$^{-/-}$) on cell viability in primary hepatic macrophages following LPS exposure (1 µg/mL, 6 h). **a** Representative flow cytometry result showing F4/80 and CD11b staining. **b** The percentages of F4/80$^+$ cells and F4/80$^+$CD11b$^+$ cells. **c** The viability of Kupffer cells in each group was determined by CCK-8 assays. Mean ± SEM of three independent experiments, $^*P < 0.05$ between the indicated groups.

[33–36]. Studies have shown that elevated aspartate transaminase (AST) and ALT in plasma are typical manifestations of liver injury. Therefore, these factors are used clinically to assess the degree of acute hepatocyte injury and early liver dysfunction [37]. In this study, the biochemical, morphological, and mechanical features of macrophages indicated that LPS administration elevated serum ALT and AST levels, disrupted the structure of liver tissue (due to profound inflammatory cell infiltration), significantly reduced macrophage viability, and prolonged the cell cycle. Furthermore, our HE staining results revealed that TLR4 deficiency reduced LPS-induced hepatic pathological changes. Protein carbonyl is an indicator of protein oxidation [38]. In our study, increased levels of protein carbonyl were observed in hepatocytes from LPS-treated mice, and this effect was abolished by TLR4 knockout. These findings suggest that TLR4 deficiency has a protective function in LPS-induced ALI.

Accumulating evidence has shown that sepsis activates the TLR4/MyD88 signaling pathway to induce NF-κB phosphorylation, leading to the secretion of many inflammatory factors [7, 39, 40]. Our current findings also indicate that TLR4 plays a vital role in the development of LPS-associated ALI [7]. When bacteria enter the circulation, they first activate the TLR4 signaling cascade and promote the transduction of target proinflammatory genes through the phosphorylation of NF-κB. This results in the release of several inflammatory factors (TNF-α, IL-6, and IL-1β), which induce apoptosis, eventually leading to liver damage and dysfunction [29]. Herein, we examined the effect of TLR4 knockout on LPS-associated ALI and the prospective molecular mechanisms. Our in vivo and in vitro results indicate that TLR4 deficiency abrogates the increases in LPS-induced TLR4 and MyD88 expression and NF-κB phosphorylation. Moreover, TLR4 deficiency attenuates LPS-mediated changes in proinflammatory cytokines (IL-6, TNF-α, and IL-1β). These findings are consistent with those of other studies indicating that TLR4/MyD88 induces hepatoprotection by modulating host immune homeostasis, thereby preventing sepsis [13, 40]. TLR4/MyD88 induces the phosphorylation of NF-κB and prevents organ damage during sepsis [30, 41, 42]. NF-κB activation was shown to overtly promote the synthesis of proinflammatory cytokines [34]. The production of proinflammatory cytokines, including TNF-α, IL-1β, and IL-6, triggers ALI. Furthermore, several studies have reported that the levels of these proinflammatory cytokines are markedly elevated in injured livers [43, 44]. Similarly, in our mouse and macrophage models of LPS-induced sepsis, we found significant increases in the protein and mRNA levels of IL-6, TNF-α, and IL-1β in hepatic cells. In contrast, the levels of these cytokines were markedly decreased in the TLR4-knockout (TLR4$^{-/-}$) group. Moreover, the variations in proinflammatory cytokines (IL-1β, IL-6, and TNF-α) coincided with the phosphorylation of NF-κB in response to LPS administration and TLR4 knockout. Briefly, these data suggest that TLR4 deficiency has a protective effect on LPS-induced inflammation in the liver.

Apoptosis plays an indispensable role in liver diseases, including cholestatic liver injury, alcoholic hepatopathy, diabetic hepatopathy, and sepsis-associated liver injury [45–48]. In sepsis, endotoxin first stimulates Kupffer cells to secrete TNF-α, which further binds to liver cells and their receptors. The resulting signal is then transduced through multiple signaling cascades, including the Fas/Apo-1 axis, TNF-α, and its receptor-mediated cascade, and the oxidant-mediated cascade. Finally, apoptotic signals are transmitted to activate caspase 3, leading to the induction of
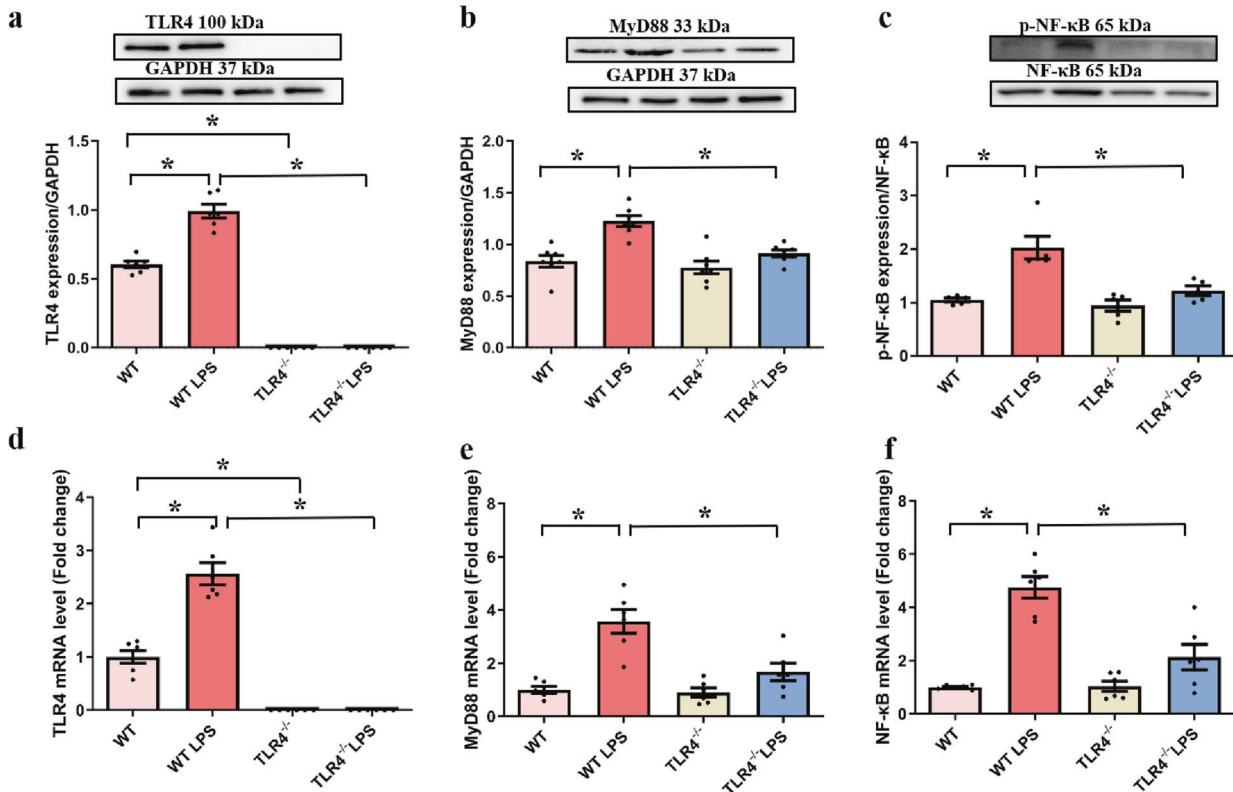
Lipopolysaccharide, TLR4, and acute liver injury
SN Chen et al.

1617

Fig. 6 Effect of TLR4 knockout (TLR4$^{-/-}$) on the protein and mRNA levels of factors involved in the TLR4/MyD88/NF-κB pathway in isolated primary hepatic macrophages following LPS exposure (1 μg/mL, 6 h). **a** The protein expression of TLR4. **b** The protein expression of MyD88. **c** The level of phosphorylated NF-κB. **d** The mRNA expression of TLR4. **e** The mRNA expression of MyD88. **f** The mRNA expression of NF-κB. Insets: Representative gel blots showing the proteins of interest (GAPDH as a loading control). Mean ± SEM, n = three independent experiments, $^*P < 0.05$ between the indicated groups.
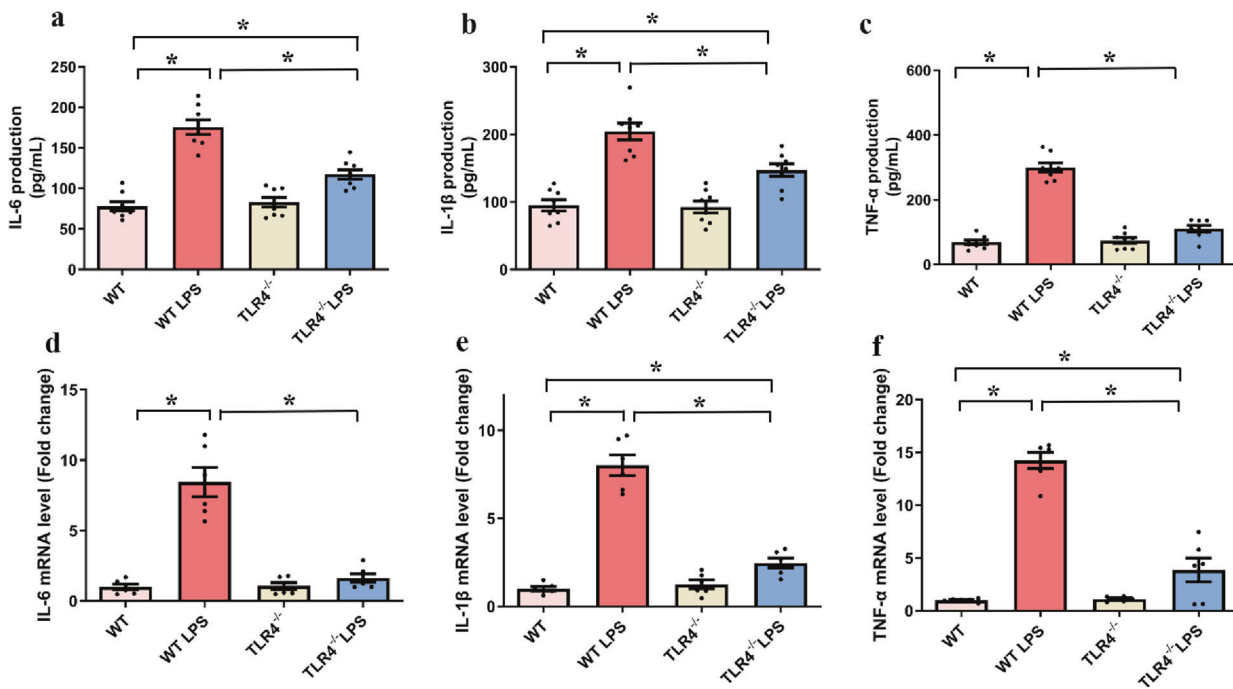

Fig. 7 Effect of TLR4 knockout (TLR4$^{-/-}$) on the protein and mRNA levels of proinflammatory cytokines in isolated primary hepatic macrophages following LPS exposure (1 μg/mL, 6 h). **a** IL-6 protein levels. **b** IL-1β protein levels. **c** TNF-α protein levels. **d** IL-6 mRNA levels. **e** IL-1β mRNA levels. **f** TNF-α mRNA levels. Mean ± SEM, n = three independent experiments, $^*P < 0.05$ between the indicated groups.

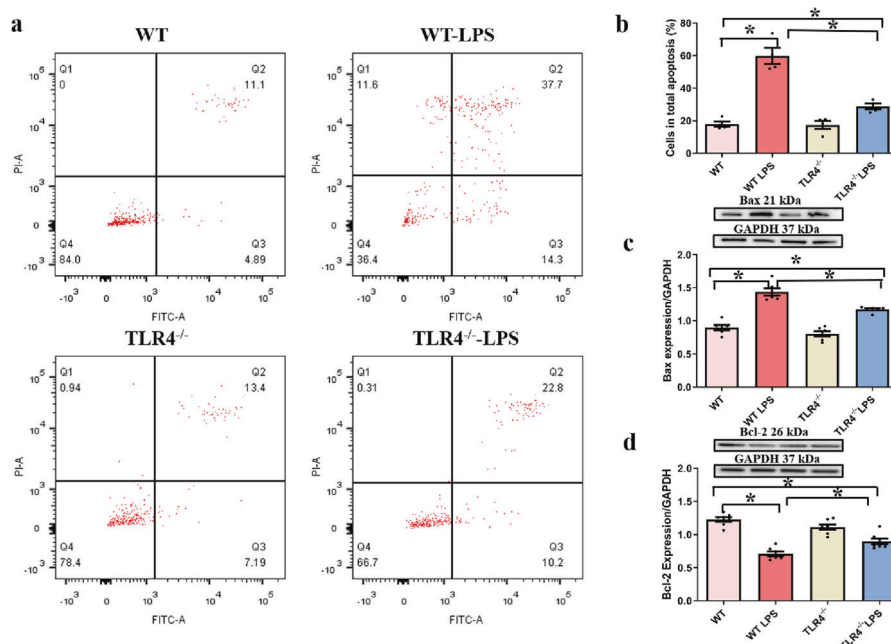Lipopolysaccharide, TLR4, and acute liver injury
SN Chen et al.

1618

Fig. 8 Effect of TLR4 knockout (TLR4$^{-/-}$) on isolated primary hepatic macrophage apoptosis following LPS exposure (1 µg/mL, 6 h). **a** RAW264.7 macrophage apoptosis was analyzed by flow cytometry. **b** Quantitative analysis of the total number of apoptotic cells in each group. **c** Bax protein expression. **d** Bcl-2 protein expression. Insets: Representative gel blots showing the proteins of interest (GAPDH as a loading control). Mean ± SEM, n = three independent experiments, $^{*}P < 0.05$ between the indicated groups.

hepatocyte apoptosis [49]. Activated caspase 3 is the chief executor of apoptosis. Moreover, studies have shown that excessive inflammation and oxidative stress caused by LPS increase liver cell apoptosis and necrosis, eventually leading to liver damage [50]. In this study, TLR4 deficiency abolished the activation of sepsis-induced inflammatory pathway and apoptosis, which was consistent with changes in proinflammatory cytokines and protein carbonyl accumulation in the liver in vitro. This was consistent with the findings of previous studies that revealed that endotoxin induces the expression of proapoptotic markers, including Bax and caspase 3, in the liver and macrophages and contributes to liver injury [8, 51]. In the present study, apoptosis levels in hepatic tissues were assessed in each group by performing TUNEL assays. Consequently, TLR4 deficiency led to a marked reduction in the number of TUNEL-positive cells in LPS-challenged mice. Earlier evidence showed that the Bcl and caspase families heavily govern the apoptotic process [52, 53]. In this study, TLR4 deficiency decreased caspase 3 activity and the expression of the apoptosis-related protein Bax. In contrast, TLR4 deficiency promoted the expression of the antiapoptotic protein Bcl-2 in LPS-induced septic mice. Moreover, our in vitro results showed that TLR4 deficiency led to a significant reduction in apoptosis in isolated primary Kupffer cells following LPS challenge. Further observations revealed that TLR4 deficiency downregulated Bax expression and upregulated Bcl-2 expression. These results reveal that TLR4 deficiency protects against LPS-induced ALI by inhibiting apoptosis.

In conclusion, our data show that TLR4 deficiency protects against LPS-induced ALI through a TLR4/MyD88/NF-κB-dependent mechanism. This mechanism involves the interplay between the activation of proinflammatory cytokines and apoptosis. TLR4 knockout alleviates liver damage by inhibiting activation of the TLR4/MyD88/NF-κB signaling cascade in macrophages, thereby reducing inflammation and apoptosis in the context of sepsis. These findings provide new insights into the identification of potential therapeutic targets to assist in the clinical management of sepsis-induced ALI.

AUTHOR CONTRIBUTIONS
SNC and YT participated in the design of experiments and manuscript preparation. XCX, QL, and QW helped with assays and analyses. YYP helped with animal care and language editing. JR and MLD supervised the experiments and manuscript preparation. All authors read and approved the final manuscript.

REFERENCES
1. Cecconi M, Evans L, Levy M, Rhodes A. Sepsis and septic shock. Lancet. 2018;392:75–87.
2. Ren J, Wu S. A burning issue: do sepsis and systemic inflammatory response syndrome (SIRS) directly contribute to cardiac dysfunction? Front Biosci. 2006;11:15–22.
3. Guo FM, Qiu HB. Definition and dignosis of sepsis 3.0. Zhonghua Nei Ke Za Zhi. 2016;55:420–32.
4. Woźnica EA, Inglot M, Woźnica RK, Łysenko L. Liver dysfunction in sepsis. Adv Clin Exp Med. 2018;27:547–51.
5. Hu C, Li L. Improvement of mesenchymal stromal cells and their derivatives for treating acute liver failure. J Mol Med. 2019;97:1065–84.
6. Strnad P, Tacke F, Koch A, Trautwein C. Liver-guardian, modifier and target of sepsis. Nat Rev Gastroenterol Hepatol. 2017;14:55–66.
7. Ding Y, Liu P, Chen ZL, Zhang SJ, Wang YQ, Cai X, et al. Emodin attenuates lipopolysaccharide-induced acute liver injury via inhibiting the TLR4 signaling pathway in vitro and in vivo. Front Pharmacol. 2018;9:962–77.
8. Jiang Z, Meng Y, Bo L, Wang C, Bian J, Deng X. Sophocarpine attenuates LPS-induced liver injury and improves survival of mice through suppressing oxidative stress, inflammation, and apoptosis. Mediators Inflamm. 2018;2018:5871431.

Lipopolysaccharide, TLR4, and acute liver injury
SN Chen et al.

1619

9. Luo Y, Fan C, Yang M, Dong M, Bucala R, Pei Z, et al. CD74 knockout protects against LPS-induced myocardial contractile dysfunction through AMPK-Skp2-SUV39H1-mediated demethylation of BCLB. Br J Pharmacol. 2020;177:1881–97.

10. Ingawale DK, Mandlik SK, Naik SR. Models of hepatotoxicity and the underlying cellular, biochemical and immunological mechanism(s): a critical discussion. Environ Toxicol Pharmacol. 2014;37:118–33.

11. Gao LN, Yan K, Cui YL, Fan GW, Wang YF. Protective effect of Salvia miltiorrhiza and Carthamus tinctorius extract against lipopolysaccharide-induced liver injury. World J Gastroenterol. 2015;21:9079–92.

12. Singh A, Koduru B, Carlisle C, Akhter H, Liu RM, Schroder K. et al. NADPH oxidase 4 modulates hepatic responses to lipopolysaccharide mediated by Toll-like receptor-4. Sci Rep. 2017;7:14346

13. Kuzmich NN, Sivak KV, Chubarev VN, Porozov YB, Savateeva-Lyubimova TN, Peri F. TLR4 signaling pathway modulators as potential therapeutics in inflammation and sepsis. Vaccines. 2017;5:34–59.

14. Tan Y, Kagan JC. A cross-disciplinary perspective on the innate immune responses to bacterial lipopolysaccharide. Mol Cell. 2014;54:212–23.

15. Medzhitov R. Approaching the asymptote: 20 years later. Immunity. 2009;30:766–75.

16. Guo J, Friedman SL. Toll-like receptor 4 signaling in liver injury and hepatic fibrogenesis. Fibrogenes Tissue Repair. 2010;3:21–40.

17. Chen Y, Wu Z, Yuan B, Dong Y, Zhang L, Zeng Z. MicroRNA-146a-5p attenuates irradiation-induced and LPS-induced hepatic stellate cell activation and hepatocyte apoptosis through inhibition of TLR4 pathway. Cell Death Dis. 2018;9:22–38.

18. Farrell GC, Haczeyni F, Chitturi S. Pathogenesis of NASH: How metabolic complications of overnutrition favour lipotoxicity and pro-Inflammatory fatty liver disease. Adv Exp Med Biol. 2018;1061:19–44.

19. Bala S, Petrasek J, Mundkur S, Catalano D, Levin I, Ward J, et al. Circulating microRNAs in exosomes indicate hepatocyte injury and inflammation in alcoholic, drug-induced, and inflammatory liver diseases. Hepatology. 2012;56:1946–57.

20. Wang Y, Chen H, Chen Q, Jiao FZ, Zhang WB, Gong ZJ. The protective mechanism of CAY10683 on intestinal mucosal barrier in acute liver failure through LPS/TLR4/MyD88 pathway. Mediators Inflamm. 2018;2018:7859601.

21. Dong M, Hu N, Hua Y, Xu X, Kandadi MR, Guo R, et al. Chronic Akt activation attenuated lipopolysaccharide-induced cardiac dysfunction via Akt/GSK3beta-dependent inhibition of apoptosis and ER stress. Biochim Biophys Acta. 2013;1832:848–63.

22. Seo HY, Kim MK, Lee SH, Hwang JS, Park KG, Jang BK. Kahweol ameliorates the liver inflammation through the Inhibition of NF-κB and STAT3 activation in primary Kupffer cells and primary hepatocytes. Nutrients. 2018;10:863–74.

23. Tsai TH, Tam K, Chen SF, Liou JY, Tsai YC, Lee YM, et al. Deletion of caveolin-1 attenuates LPS/GalN-induced acute liver injury in mice. J Cell Mol Med. 2018;22:5573–82.

24. Guo R, Xu X, Babcock SA, Zhang Y, Ren J. Aldehyde dedydrogenase-2 plays a beneficial role in ameliorating chronic alcohol-induced hepatic steatosis and inflammation through regulation of autophagy. J Hepatol. 2015;62:647–56.

25. Suzuki S, Toledo-Pereyra LH, Rodriguez FJ, Cejalvo D. Neutrophil infiltration as an important factor in liver ischemia and reperfusion injury. Modulating effects of FK506 and cyclosporine. Transplantation. 1993;55:1265–72.

26. Zhao P, Wang J, He L, Ma H, Zhang X, Zhu X, et al. Deficiency in TLR4 signal transduction ameliorates cardiac injury and cardiomyocyte contractile dysfunction during ischemia. J Cell Mol Med. 2009;13:1513–25.

27. Guo R, Zhong L, Ren J. Overexpression of aldehyde dehydrogenase-2 attenuates chronic alcohol exposure-induced apoptosis, change in Akt and Pim signalling in liver. Clin Exp Pharmacol Physiol. 2009;36:463–8.

28. Ren J, Xu X, Wang Q, Ren SY, Dong M, Zhang Y. Permissive role of AMPK and autophagy in adiponectin deficiency-accentuated myocardial injury and inflammation in endotoxemia. J Mol Cell Cardiol. 2016;93:18–31.

29. Luedde T, Schwabe RF. NF-κB in the liver-linking injury, fibrosis and hepatocellular carcinoma. Nat Rev Gastroenterol Hepatol. 2011;8:108–18.

30. Zi SF, Li JH, Liu L, Deng C, Ao X, Chen DD, et al. Dexmedetomidine-mediated protection against septic liver injury depends on TLR4/MyD88/NF-κB signaling downregulation partly via cholinergic anti-inflammatory mechanisms. Int Immunopharmacol. 2019;76:105898.

31. Endo-Umeda K, Nakashima H, Komine-Aizawa S, Umeda N, Seki S, Makishima M. Liver X receptors regulate hepatic F4/80$^+$CD11b$^+$ Kupffer cells/macrophages and innate immune responses in mice. Sci Rep. 2018;8:9281.

32. Jirillo E, Caccavo D, Magrone T, Piccigallo E, Amati L, Lembo A, et al. The role of the liver in the response to LPS: experimental and clinical findings. J Endotoxin Res. 2002;8:319–27.

33. Liu Y, Zhu Y, Wang Y, Wan C. Differences between congenital-syphilis presenting as sepsis and neonatal sepsis: a case-control study. Med (Baltim). 2019;98:e17744.

34. Li XH, Wu MJ, Zhang LN, Zheng JJ, Zhang L, Wan JY. Effects of polydatin on ALT, AST, TNF-alpha, and COX-2 in sepsis model mice. Zhongguo Zhong Xi Yi Jie He Za Zhi. 2013;33:225–8.

35. Wu M, Chen W, Yu X, Ding D, Zhang W, Hua H, et al. Celastrol aggravates LPS-induced inflammation and injuries of liver and kidney in mice. Am J Transl Res. 2018;10:2078–86.

36. Zhu J, Lin X, Yan C, Yang S, Zhu Z. microRNA-98 protects sepsis mice from cardiac dysfunction, liver and lung injury by negatively regulating HMGA2 through inhibiting NF-κB signaling pathway. Cell Cycle. 2019;18:1948–64.

37. Jia X, Iwanowycz S, Wang J, Saaoud F, Yu F, Wang Y, et al. Emodin attenuates systemic and liver inflammation in hyperlipidemic mice administrated with lipopolysaccharides. Exp Biol Med. 2014;239:1025–35.

38. Ibitoye R, Kemp K, Rice C, Hares K, Scolding N, Wilkins A. Oxidative stress-related biomarkers in multiple sclerosis: a review. Biomark Med. 2016;10:889–902.

39. Rosadini CV, Kagan JC. Early innate immune responses to bacterial LPS. Curr Opin Immunol. 2017;44:14–9.

40. Zhou L, Liu Z, Wang Z, Yu S, Long T, Zhou X, et al. Astragalus polysaccharides exerts immunomodulatory effects via TLR4-mediated MyD88-dependent signaling pathway in vitro and in vivo. Sci Rep. 2017;7:44822.

41. Shen N, Cheng A, Qiu M, Zang G. Allicin improves lung injury induced by sepsis via regulation of the Toll-like receptor 4 (TLR4)/myeloid differentiation primary response 88 (MYD88)/nuclear factor kappa B (NF-κB) pathway. Med Sci Monit. 2019;25:2567–76.

42. Jin YH, Li ZT, Chen H, Jiang XQ, Zhang YY, Wu F. Effect of dexmedetomidine on kidney injury in sepsis rats through TLR4/MyD88/NF-κB/iNOS signaling pathway. Eur Rev Med Pharmacol Sci. 2019;23:5020–5.

43. Campana L, Starkey Lewis PJ, Pellicoro A, Aucott RL, Man J, O'Duibhir E, et al. The STAT3-IL-10-IL-6 pathway is a novel regulator of macrophage efferocytosis and phenotypic conversion in sterile liver injury. J Immunol. 2018;200:1169–87.

44. Lu H, Zhang L, Gu LL, Hou BY, Du GH. Oxymatrine induces liver injury through JNK signalling pathway mediated by TNF-α in vivo. Basic Clin Pharmacol Toxicol. 2016;119:405–11.

45. Yamada S, Noguchi H, Tanimoto A. Critical and diverse in vivo roles of apoptosis signal-regulating kinase 1 in animal models of atherosclerosis and cholestatic liver injury. Histol Histopathol. 2017;32:433–44.

46. Oami T, Watanabe E, Hatano M, Teratake Y, Fujimura L, Sakamoto A, et al. Blocking liver autophagy accelerates apoptosis and mitochondrial injury in hepatocytes and reduces time to mortality in a murine sepsis model. Shock. 2018;50:427–34.

47. Petrović A, Bogojević D, Korać A, Golić I, Jovanović-Stojanov S, Martinović V, et al. Oxidative stress-dependent contribution of HMGB1 to the interplay between apoptosis and autophagy in diabetic rat liver. J Physiol Biochem. 2017;73:511–21.

48. Menk M, Graw JA, Poyraz D, Möbius N, Spies CD, von Haefen C. Chronic alcohol consumption inhibits autophagy and promotes apoptosis in the liver. Int J Med Sci. 2018;15:682–8.

49. Brenner C, Galluzzi L, Kepp O, Kroemer G. Decoding cell death signals in liver inflammation. J Hepatol. 2013;59:583–94.

50. Zhong W, Qian K, Xiong J, Ma K, Wang A, Zou Y. Curcumin alleviates lipopolysaccharide induced sepsis and liver failure by suppression of oxidative stress-related inflammation via PI3K/AKT and NF-κB related signaling. Biomed Pharmacother. 2016;83:302–13.

51. Ju M, Liu B, He H, Gu Z, Liu Y, Su Y, et al. MicroRNA-27a alleviates LPS-induced acute lung injury in mice via inhibiting inflammation and apoptosis through modulating TLR4/MyD88/NF-κB pathway. Cell Cycle. 2018;17:2001–18.

52. Fan TJ, Han LH, Cong RS, Liang J. Caspase family proteases and apoptosis. Acta Biochim Biophys Sin. 2005;37:719–27.

53. Borner C. The Bcl-2 protein family: sensors and checkpoints for life-or-death decisions. Mol Immunol. 2003;39:615–47.